



Cite this: RSC Adv., 2018, 8, 3081

Received 10th November 2017  
 Accepted 8th January 2018

DOI: 10.1039/c7ra12307h  
[rsc.li/rsc-advances](http://rsc.li/rsc-advances)

## 1. Introduction

Lignocellulosic fiber, being degradable and renewable, has been widely used in many areas, such as paper and paperboard products,<sup>1</sup> high-temperature fiber composites<sup>2</sup> and so on. The fiber surface wettability is thought to be essential for fiber swelling, the ability of the fiber volume to become larger during the wetting process, which is good for the interface contact of two fibers so that the bonding properties could be improved.<sup>3</sup> Further, the fiber surface wettability can have an influence on the bonding strength between two fibers in a fiber network (paper and paperboard products) by affecting fiber surface composition and functional groups. However, the lignocellulosic fiber surface wettability has seldom been seriously taken into consideration.

Fiber surface wettability is defined as the ability for a kind of liquid to spread onto the fiber surface, which is consisted of surface composites, surface charge, surface free energy and many other kinds of surface properties related to fiber surface wetting process.<sup>4</sup> Lignocellulosic fiber is composed of hydrophilic part (carbohydrates, including cellulose and hemicelluloses) and hydrophobic part (lignin and some of the extractives). During the separation from natural plants, fibers were treated with different kinds of methods, either mechanical or chemical, mainly to compromise the relationship between

lignin and carbohydrates so that the fiber surface wettability could be improved.

The inter-fiber bonding strength of the fiber network, originating from the hydrogen bonding and the van der Waals' force,<sup>5</sup> is one of the most important characteristics influencing the final products. The inter-fiber bonding, especially the hydrogen bonding, is largely dependent on the surface wettability.<sup>6</sup> The fiber surface composition, including cellulose, hemicellulose, lignin and some extractives, has a strong influence on the inter-fiber bonding properties.<sup>7</sup> It has been proved that the lignin on the fiber surface would have a bad effect on the inter-fiber bonding because the lignin is hydrophobic compared to carbohydrates. However, the phenolic group associated with lignin is proved to be one of the resources of the fiber surface charge,<sup>8</sup> which has a non-ignorable influence on the inter-fiber bonding strength.<sup>9</sup> The improvement of surface charge can increase the inter-fiber bonding mainly by influencing the inter-fiber hydrogen bonding according to Araci *et al.*<sup>10</sup> Furthermore, the decrease of the surface lignin can also lead to the final yield sacrificing of the lignocellulosic fibers. As a result, a large amount of studies have been done focusing on the modification of lignin instead of removing it,<sup>11,12</sup> which can improve the wettability of the fiber surface so that the inter-fiber bonding could be enhanced. Fiber surface free energy and contact angle are always used as the evaluation of the fiber surface wettability.<sup>13</sup> The fiber surface free energy has a vital influence on fiber swelling, assistance, and inter-fiber contact. However, there are very few literatures concerning about lignocellulosic fiber surface free energy.

In this study, the lignin-rich fiber will be subjected to mechanical refining in order to modify the fiber surface

<sup>a</sup>Tianjin Key Lab of Pulp & Paper, Tianjin University of Science & Technology, Tianjin, 300457 China. E-mail: [hongjiezhang@tust.edu.cn](mailto:hongjiezhang@tust.edu.cn); Fax: +86-22-6060-2510; Tel: +86-22-6060-2199

<sup>b</sup>Hebei Huatai Paper Industry Co. Ltd., Huatai Group, Zhaoxian, 051530 China

<sup>c</sup>Shandong Huatai Paper Industry Co. Ltd., Huatai Group, Dongying, 257335 China

wettability, and the fiber surface lignin, surface charge and surface free energy would be determined respectively to evaluate the fiber surface wettability. Also, the inter-fiber bonding capability, as well as physical performances of handsheets, would be measured. The main objective of this study is to improve the bonding capability of fiber matrix by improving the fiber surface wettability. The relationship between fiber surface wettability and the inter-fiber bonding strength will also be investigated so that the final product properties could be better adjusted without much sacrifice of the energy and materials during the papermaking process.

## 2. Materials and methods

### 2.1 Materials

The pine thermo-mechanical pulp (TMP) fiber, provided by a paper mill in Hebei province in China, was classified by using Bauer-McNutt fiber classifier (TMI 8901-5, USA) into different fiber fractions. The R30 fiber fraction with the length of 2.4–2.6 mm and width of 40.1–40.5  $\mu\text{m}$  was chosen as the raw material to be treated by mechanical refining. A PFI mill (Frank-PTI, Germany) was used with a fiber consistency of 30%. The revolution for refining was 0 r, 5000 r, 10 000 r, 13 000 r and 15 000 r, respectively. After refining, the fiber was classified and the R30 fraction was collected for further experiments.

### 2.2 Fiber surface wettability

The fiber surface lignin content was analyzed by using a PHI-1600 X-ray photoelectron spectrometer (XPS), in accordance with Li and Reeve.<sup>14</sup>

The fiber surface charge was determined through polyelectrolyte adsorption method by using high molecular weight poly-DADMAC ( $2\text{--}3.5 \times 10^5 \text{ g mol}^{-1}$ ), as reported by Zhang *et al.*<sup>15</sup>

The surface free energy of the fiber was detected based on the contact angle measurement.<sup>16</sup> Two fibers of a similar diameter were put in a parallel way onto a manmade slide. And the contact angle measurement of the fibers was manufactured by putting a liquid drop onto the gap of 0.1–0.3 mm between them. Two kinds of liquids were applied in this study (water and glycerol).

The surface free energy was calculated according to eqn (1) and (2).<sup>17</sup>

$$\gamma_s = \gamma_s^D + \gamma_s^d \quad (1)$$

$$\gamma_L(1 + \cos \theta) = 2\sqrt{\gamma_s^d \gamma_L^d} + 2\sqrt{\gamma_s^D + \gamma_L^D} \quad (2)$$

where  $\gamma_s$  is the surface free energy of the fiber ( $\text{mJ m}^{-2}$ ),  $\gamma_L$  is the surface free energy of the liquid used ( $\text{mJ m}^{-2}$ ),  $\gamma_s^d$  is the dispersion component of the liquid surface free energy ( $\text{mJ m}^{-2}$ , 52.2  $\text{mJ m}^{-2}$  for water and 41.5  $\text{mJ m}^{-2}$  for glycerol),  $\gamma_L^D$  is the no dispersion component of the liquid surface free energy ( $\text{mJ m}^{-2}$ , 19.9  $\text{mJ m}^{-2}$  for water and 21.2  $\text{mJ m}^{-2}$  for glycerol),  $\gamma_s^D$  and  $\gamma_s^d$  is the dispersion and no dispersion component of the fiber surface free energy ( $\text{mJ m}^{-2}$ ),  $\theta$  is the contact angle of the liquid onto the fiber.

### 2.3 Fiber characterization

**2.3.1 Fiber morphology.** The fiber morphology (including the fiber length, fiber width and coarseness) was determined by the fiber tester (912, Sweden Lorentzen&Wettre) based on the ISO 16065-2 national standard.

**2.3.2 AFM observation of fiber surface.** A small dose of fibers were suspended in distilled water in a concentration of 0.4%. Two drops of the suspension were dropped onto a mica sheet and air dried. Then the sample was fixed onto the object stage of the AFM and imaged. The JSPM 5200 atomic force microscope (AFM) was used in this work. The tapping model was chosen and the elastic constant of the cantilevers was  $3.2 \text{ N m}^{-1}$ . The cantilevers length and the radius of curvature of the probe were 450  $\mu\text{m}$  and 5–10  $\mu\text{m}$ , respectively. Ten samples were tested for each kind of fibers and the two dimensional graphs were chosen as the final images for the analysis of the fiber surface.

**2.3.3 "Water capacity".** The water retention value (WRV) was determined by the centrifuge method as the expression of "water capacity". About 0.15 g of fiber sample was suspended into 15 mL of distilled water and removed into a cylinder (with 100-mesh wire). The fibers were then centrifuged at 2500 rpm for 20 min with the centrifuge (3-16PK, Sigma). The centrifuged fibers were weighed before and after over 12 h of drying at 105 °C. The WRV was calculated by eqn (3).

$$\text{WRV\%} = [(\text{wet weight} - \text{dry weight})/\text{dry weight}] \times 100 \quad (3)$$

**2.3.4 Fiber flexibility.** The fiber flexibility was determined based on Steadman and Luner's study.<sup>18</sup> The fibers were diluted into distilled water with a consistency of 0.01% and shaped onto a 200 mesh filter cloth with the TAPPI standard handsheet former (Lab Tech, Canada). And then the fiber sheet was pressed with two slides with stainless steel wires (diameter, 35  $\mu\text{m}$ ) in advance using a standard handsheet press (no. 2571-1, KRK, Japan) for 5 min at 420 kPa with two press felts on each side. The slides were then removed from the cloth and air-dried for 8 h at room temperature. A light optical microscope with a CCD camera was then utilized for the imaging of the dried fibers that are perpendicular to the wires. The fiber images in accompany with the instrument were used for the measurement of the free span length (fiber length not in contact with the slide) and the fiber width. And the final result was calculated through the eqn (4).

$$F = 72d/qL^4 \quad (4)$$

where  $F$  is the fiber flexibility;  $d$  is the deflection height (wire diameter, 35  $\mu\text{m}$ );  $q$  is the pressing load,  $\text{N m}^{-1}$ , based on the fiber width (m) and the pressure; and  $L$  is the free span length (m).

**2.3.5 The ATR-FTIR characterization.** The fiber surface groups were characterized by Attenuated Total Reflection Fourier transformed Infrared Spectroscopy (ATR-FTIR) 920 in 25 °C and 65% RH. The measurement was performed by a ceramic infrared light source in a scanning speed of 2  $\text{mm S}^{-1}$ . For each sample, the range chosen was from 4000 to 600  $\text{cm}^{-1}$  with a resolution of 1  $\text{cm}^{-1}$ .

## 2.4 Physical properties and inter-fiber bonding capability

The fibers were then made into handsheets according to the TAPPI Test Method T205 sp-95 for the determination of physical properties. The tensile strength was tested with a tensile tester (L&W 004, Sweden), and the zero-span tensile strength was detected by a Z-span tester (PULMAC 2400, USA), based on the TAPPI Method T220 sp-96. The bonding strength index (B) was calculated by eqn (5).<sup>19</sup>

$$1/T = 9/8/Z + 1/B \quad (5)$$

where  $T$  is the tensile index ( $\text{N m g}^{-1}$ ),  $Z$  is the zero-span tensile index ( $\text{N m g}^{-1}$ ),  $B$  is the bonding strength index ( $\text{N m g}^{-1}$ ).

## 2.5 Relative bonded area (RBA) detection

The RBA between fibers were detected through the BET adsorption method according to Soszynski's study.<sup>20</sup> The specific surface area of the fiber and the handsheet were tested using the BET method and the RBA was calculated by eqn (6).

$$\text{RBA} = (A_0 - A)/A_0 \quad (6)$$

where  $A_0$  is the specific surface area of the free fiber ( $\text{m}^2 \text{ g}^{-1}$ ),  $A$  is the specific surface area of the handsheet ( $\text{m}^2 \text{ g}^{-1}$ ).

## 3. Results and discussion

Lignocellulosic fiber, a cylinder-shaped material as shown in the SEM image in Fig. 1, is a kind of a "water battery", where, the "hydrolyte solution" (a solution of surface composition and surface functional groups) plays a major role in the wetting process of fiber surface (in Fig. 1). The "water capacity" is used for the evaluation of bound water the lignocellulosic fiber could adsorb and maintain, which strongly contributes to the fiber swelling and flexibility. The fiber surface wettability, including surface constituents, surface charge, surface free energy and so on, could be seen as a switch accommodating the "water capacity" by getting the fiber "water charged" with different kinds of hydrophilic groups, which further increase the

Table 1 The surface lignin of treated fibers

Treatment (rev.)	O/C (%)	Surface lignin (%)
0	39.7 ± 0.1	87.1 ± 0.1
5000	40.0 ± 0.1	86.7 ± 0.1
10 000	42.4 ± 0.2	81.9 ± 0.1
13 000	42.5 ± 0.1	81.5 ± 0.1
15 000	44.6 ± 0.3	77.5 ± 0.1

hydrogen bonding between fibers. The process could be expressed by surface contact angle and surface free energy.

### 3.1 Surface lignin and surface wettability

The fiber surface composition is the main solute of the "hydrolyte solution". Fiber surface wettability is mainly dominated by the surface composition, including the hydrophilic carbohydrates and hydrophobic lignin.

It's known that there're large amounts of hydroxyl and carboxyl groups in cellulose and hemicellulose structures,<sup>21,22</sup> which makes carbohydrates hydrophilic. By contrast, lignin, with a considerable quantity of benzene structures, is more hydrophobic than carbohydrates and the fiber wettability is restricted by surface lignin to a great extent. However, thanks to its structure, lignin has a large rigidity and is known as the support of the lignocellulosic fiber, spacing among other kinds of compositions, which contributes to the high bulk of paper or paperboard products made from lignin-rich fibers. The amount of the surface lignin during the refining process is shown in Table 1.

It can be seen in Table 1 that the surface lignin decreased from 87.1% to 77.5% with the increase of the PFI revolutions. That may be caused by the peeling effect of the refining process.<sup>5,23</sup> The decrease of the surface lignin will lead to a better explosion of carbohydrates, resulting in a more hydrophilic surface and larger surface wettability. In addition, the decrease of surface lignin may have a positive effect on the inter-fiber bonding because of the improvement of the fiber softness and swelling. However, the phenolic groups associated with lignin are one of the resources of the fiber surface charge.

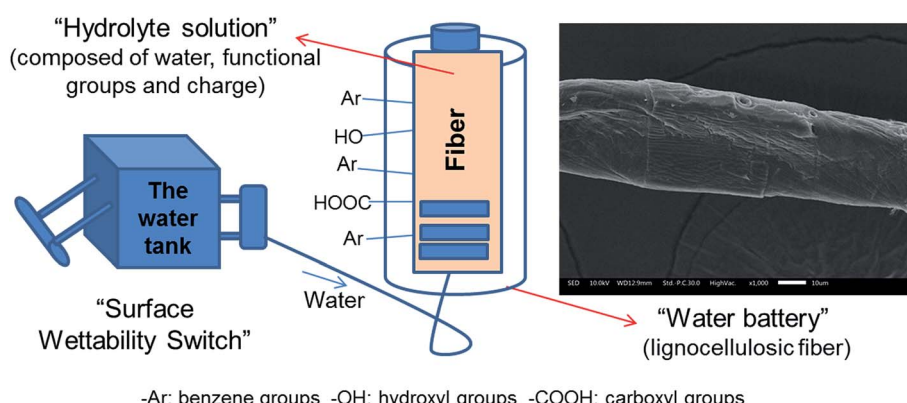


Fig. 1 Schematic diagram for the "water-charged" degree of lignocellulosic fiber (water battery) switched by the fiber surface wettability.



Table 2 The polarity of some functional groups<sup>a</sup>

Polarity	increasing		
Functional groups	Hydroxyl	Phenolic hydroxyl	Carboxyl
Chemical formula	-OH	Ar-OH	-COOH

<sup>a</sup> Ar is the benzene group.

Table 3 Characterization of surface charge

Treatment (rev.)	Samples	Surface charge (mmol kg <sup>-1</sup> )
0	0#	48.38 ± 0.8
5000	1#	51.04 ± 0.6
10 000	2#	54.69 ± 0.4
13 000	3#	56.60 ± 0.3
15 000	4#	60.38 ± 0.5

As a result, the surface charge might be negatively influenced by the decrease of surface lignin.

### 3.2 Surface charge and surface wettability

Fibers are charged when suspended into water because of their anionic groups from different kinds of surface compositions, such as carboxyl groups. Fiber charge includes surface charge and total charge. The total charge consists of surface and inner charge.<sup>20</sup> The surface charge is one of the most important parameters for fiber, especially for its swelling, bonding and the properties of the final products. The surface charge is mainly caused by the anionic groups on fiber surface,<sup>24</sup> including the carboxyl groups from hemicellulose and phenolic groups associated with lignin and many other kinds of functional groups. These functional groups existing in the "hydrolyte solution" are the major ingredients to retain water molecules. The comparison of the polarity of some different kinds of functional groups is listed in Table 2.

The surface charge of the treated fibers was shown in Table 3. It can be seen in Table 3 that during the mechanical treatment, the surface charge increased from 48.38 mmol kg<sup>-1</sup> to 60.38 mmol kg<sup>-1</sup>. That might be caused by the increase of the fiber specific surface area, which was due to the fiber fibrillation.<sup>25</sup> Further, the increase of the specific surface area can also result in the increase of the accessibility of the polyelectrolyte during the surface charge determination. Moreover, the decrease of the surface lignin could improve the exposure of the

carbohydrates on the fiber surface so that many other anionic groups on the carbohydrates would be exposed, which may have a positive effect on the increase of the surface charge. As shown in Table 2, carboxyl groups have a higher polarity compared with many other functional groups, which can better constrain the water<sup>26</sup> and increase the fiber surface wettability. Further, the fiber surface functional groups and surface charge may be good for the inter-fiber bonding strength by influencing the inter-fiber bonding force, especially the hydrogen bonding strength.

### 3.3 Surface free energy and surface wettability

The surface contact angle and surface free energy of different kinds of mechanically treated fibers were listed in Table 4, which was calculated based on the eqn (2).

Table 4 shows that the fiber surface free energy has an enhancement of nearly 10 mJ m<sup>-2</sup> with the PFI revolutions ranging from 0 r to 15 000 r, indicating the increase of the surface wettability. That increase may be caused by the improvement of the surface charge and the decrease of the surface lignin, which can have a positive effect on the surface wettability since lignin is more hydrophobic than carbohydrates.<sup>27</sup> The increase of surface charge is mainly caused by the fibrillation of the fibers, which exposes more carbohydrates,<sup>28</sup> leading to the improvement of fiber surface wettability.

### 3.4 Surface wettability and the inter-fiber bonding properties

Fiber surface wettability has a strong influence on the inter-fiber bonding strength. The inter-fiber bonding strength has been conducted by Page as bonding strength index (*B*), which is decided by a group of parameters. The calculation of *B* is shown in eqn (7).

$$B = P \times l \times b \times \text{RBA}/12/g/C \quad (7)$$

where *P* is the fiber perimeter (m), *l* is the fiber length (m), *b* is the fiber-fiber bonding strength (N m<sup>-2</sup>), *g* is the gravitational constant (9.8 m s<sup>-2</sup>), *C* is the fiber coarseness (g m<sup>-1</sup>).

According to eqn (7), when the fibers are fixed, the inter-fiber bonding strength mainly lies on the RBA and the *b* of two fibers.

**3.4.1 Fiber surface wettability and inter-fiber relative bonded area (RBA).** The RBA of two fibers is decided by the mechanical properties of fibers, such as the fiber specific surface area,<sup>29</sup> fiber flexibility,<sup>30</sup> WRV and so on. Fibers with

Table 4 The contact angle and surface free energy of mechanically treated fibers<sup>a</sup>

Treatment (rev.)	WCA (degree)	GCA (degree)	$\gamma_s^d$ (mJ m <sup>-2</sup> )	$\gamma_s^D$ (mJ m <sup>-2</sup> )	$\gamma_s$ (mJ m <sup>-2</sup> )
0	60.30 ± 0.50	50.00 ± 0.40	16.66 ± 0.10	29.97 ± 0.24	46.63 ± 0.33
5000	52.53 ± 0.30	42.49 ± 0.30	28.07 ± 0.02	19.51 ± 0.09	47.58 ± 0.11
10 000	56.32 ± 0.30	45.43 ± 0.30	19.59 ± 0.03	29.09 ± 0.11	48.69 ± 0.13
13 000	48.86 ± 0.20	38.52 ± 0.20	32.78 ± 0.00	17.02 ± 0.05	49.80 ± 0.04
15 000	43.24 ± 0.10	33.26 ± 0.10	44.23 ± 0.01	10.22 ± 0.02	54.45 ± 0.01

<sup>a</sup> WCA – water contact angle; GCA – glycerol contact angle.

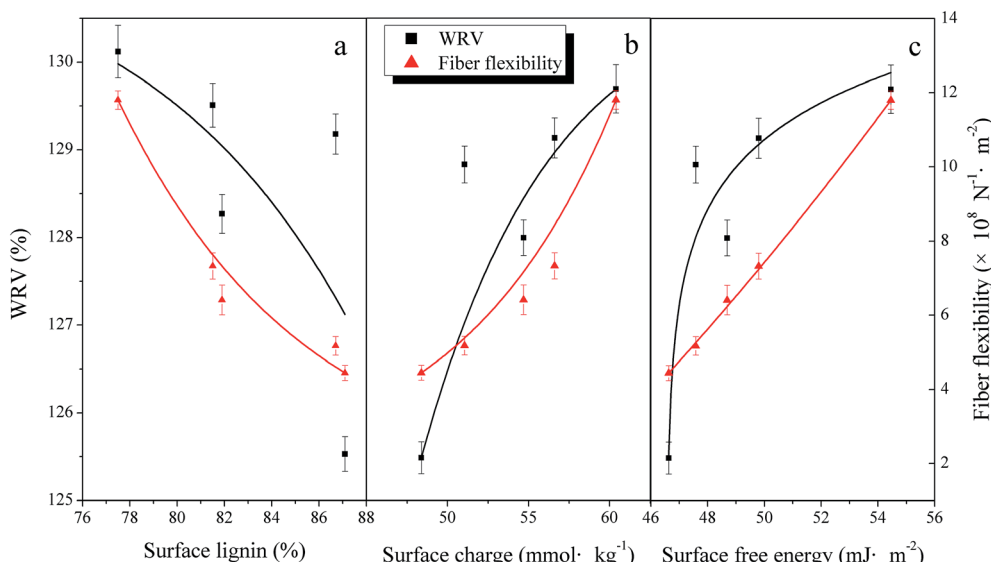


Fig. 2 Relationship between fiber surface wettability and WRV and fiber flexibility.

a good flexibility and WRV could have more chances to contact with each other, meaning that the inter-fiber bonding area would increase. Similar results have been found in the study of Li *et al.*<sup>18</sup> Furthermore, the WRV of the fibers and the bonding area had a positive correlation with each other, which has been in association with Tao *et al.*<sup>31</sup>

The fiber flexibility is the fiber deflection of unit length under unit load.<sup>32</sup> During the papermaking process, the fiber deflection will make the fibers bond more tightly and both the RBA and the hydrogen bonding between two fibers will increase.<sup>33</sup> Improving the fiber WRV makes for the fiber swelling, which is also good for the fiber flexibility increasing. The relationships between fiber surface wettability and the fiber flexibility and the WRV are shown in Fig. 2.

Fig. 2 shows that both fiber flexibility and WRV increased ( $4.44 \times 10^8 \text{ N}^{-1} \text{ m}^{-2}$  to  $1.18 \times 10^9 \text{ N}^{-1} \text{ m}^{-2}$  and 125.53% to 130.12%, respectively) with the improvement of surface wettability, surface lignin (87.1% to 77.5%), surface charge (48.38 mmol kg<sup>-1</sup> to 60.38 mmol kg<sup>-1</sup>) and surface free energy (46.63 mJ m<sup>-2</sup> to 54.45 mJ m<sup>-2</sup>). The increase of WRV was due to the fact that the fiber surface became more hydrophilic during the mechanical treatment in accordance with the improvement of the surface free energy. The decrease of surface lignin could lead to the explosion of carbohydrates, which are much more hydrophilic so that the surface wettability increased to an extent.<sup>33</sup> The improvement of the pore size and surface charge during the refining process also led to the WRV increase<sup>34</sup> by facilitating fiber swelling. The fiber surface charge mainly comes from the functional groups on the fiber surface,

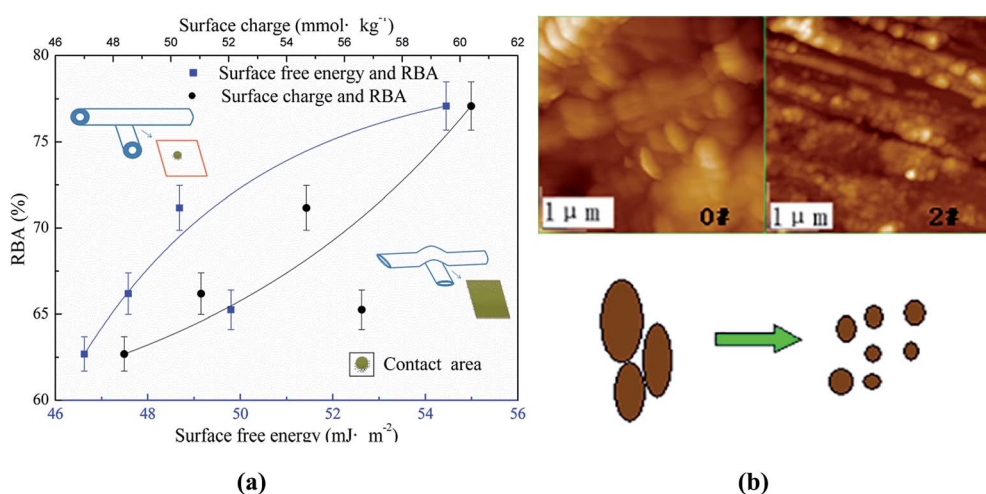


Fig. 3 (a) The relationship between RBA and the surface wettability (insert: the sketch of fiber flexibility and RBA improvement during the mechanical PFI modification); (b) the AFM graphs of fiber surface lignin (0#: mechanical PFI revolution of 0 r; 2#: mechanical PFI revolution of 10 000 r).

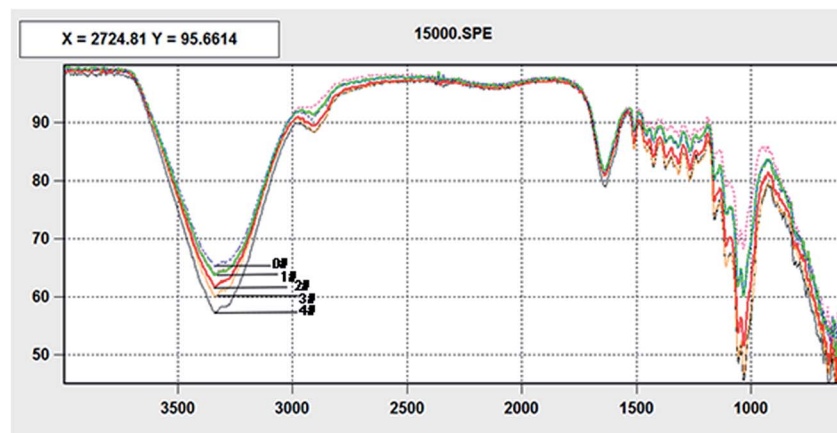


Fig. 4 FTIR spectra of the mechanically treated fibers.

such as the carboxyl groups, which are hydrophilic with a high polarity as seen in Table 2 and can strengthen the fiber swelling ability.

In addition, fiber swelling can also promote the fiber flexibility since swelled fiber is much softer than before. During the surface free energy increasing, the fiber swelling could happen more easily, which increased the flexibility of the fibers.<sup>35</sup> Lignin is one of the most important factors restricting the fiber flexibility with a stiff structure.<sup>36</sup> The inter-fiber bonding strength is limited accordingly. It's reported<sup>8</sup> that the surface lignin of TMP fibers accounted for over 25–35% of the total lignin, indicating that the surface lignin plays an especially important role in the fiber flexibility. As a result, the decrease of surface lignin could be beneficial for the fiber flexibility increase.

Above all, it can be concluded that the fiber surface wettability could contribute to the improvement of the RBA between two fibers, which can be seen more clearly in Fig. 3.

It's obvious in Fig. 3(a) that the RBA rose from 62.69% to 77.08% with the improvement of both the surface charge and free energy. As discussed before, when the fiber surface charge and surface free energy increased, the fiber became more

flexible and more easily wetted, which gained a tighter inter-fiber bonding during the papermaking process. This can also be seen in Fig. 3(a). In Fig. 3(b), the lignin fragment changed into smaller ones during the mechanical treatment, which exposed more carbohydrates with more anionic groups, whose high polarity facilitated the inter-fiber bonding. In addition, it could be seen in Fig. 3(b) that the fiber surface roughness increased after the mechanical treatment, which was caused by the fragmentation of lignin structure and the explosion of micro fibrils.<sup>37</sup> This means that the fiber specific surface area enlarged<sup>38</sup> so that there were more chances for fibers to contact with each other. It can be concluded that fiber surface wettability is a group of valuable characteristics in adjusting the fiber contact area of the final products.

**3.4.2 Fiber surface wettability and inter-fiber bonding strength (*b*).** It's reported<sup>39</sup> that the inter-fiber bonding strength is related to the specific bonding strength (*b*), which means the strength and the amount of the hydrogen bonding for each two bonding fibers. The *b* is mainly supported by the hydrogen bonding between two fibers, which is based on the hydrophilic groups on the fiber surface. Reasonably, the surface groups of the treated fibers were analyzed by FTIR and shown in Fig. 4.

According to Fig. 4, the difference among five kinds of fibers is mainly the difference of the group consistency. The band at around  $3422\text{ cm}^{-1}$  that changed most during the refining process is proved to be the hydroxyl groups,<sup>40</sup> which can form more hydrogen bonds between fibers. This might be due to the explosion of the carbohydrates during the refining process, which has a peeling effect on the fiber surface lignin.<sup>41</sup> Furthermore, it has been discussed before that the explosion of the surface carbohydrates, especially the hemicellulose, could also induce the increase of the surface carboxyl groups. Hydrogen bonds can also be formed between carboxyl and hydroxyl (or carboxyl) groups.<sup>42,43</sup> The relationship between fiber surface wettability and *b* is shown in Fig. 5.

It could be seen in Fig. 5 that the *b* rose from  $7.5\text{ N m}^{-2}$  to  $11.3\text{ N m}^{-2}$  with the improvement of both the surface charge and surface free energy. The improvement of the surface charge contributes to the hydrogen bonding between fibers own to the

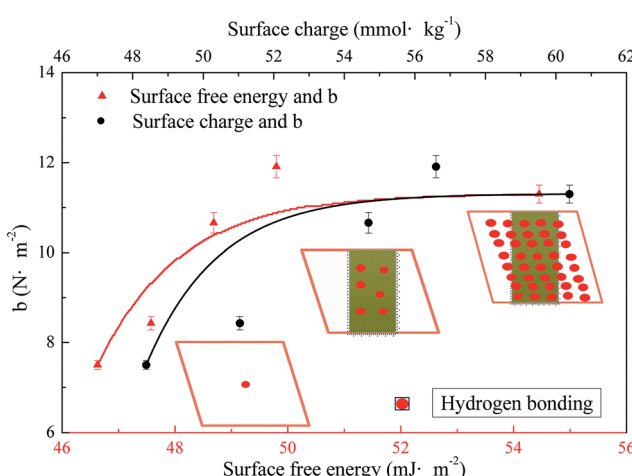


Fig. 5 Relationship between *b* and the surface properties.



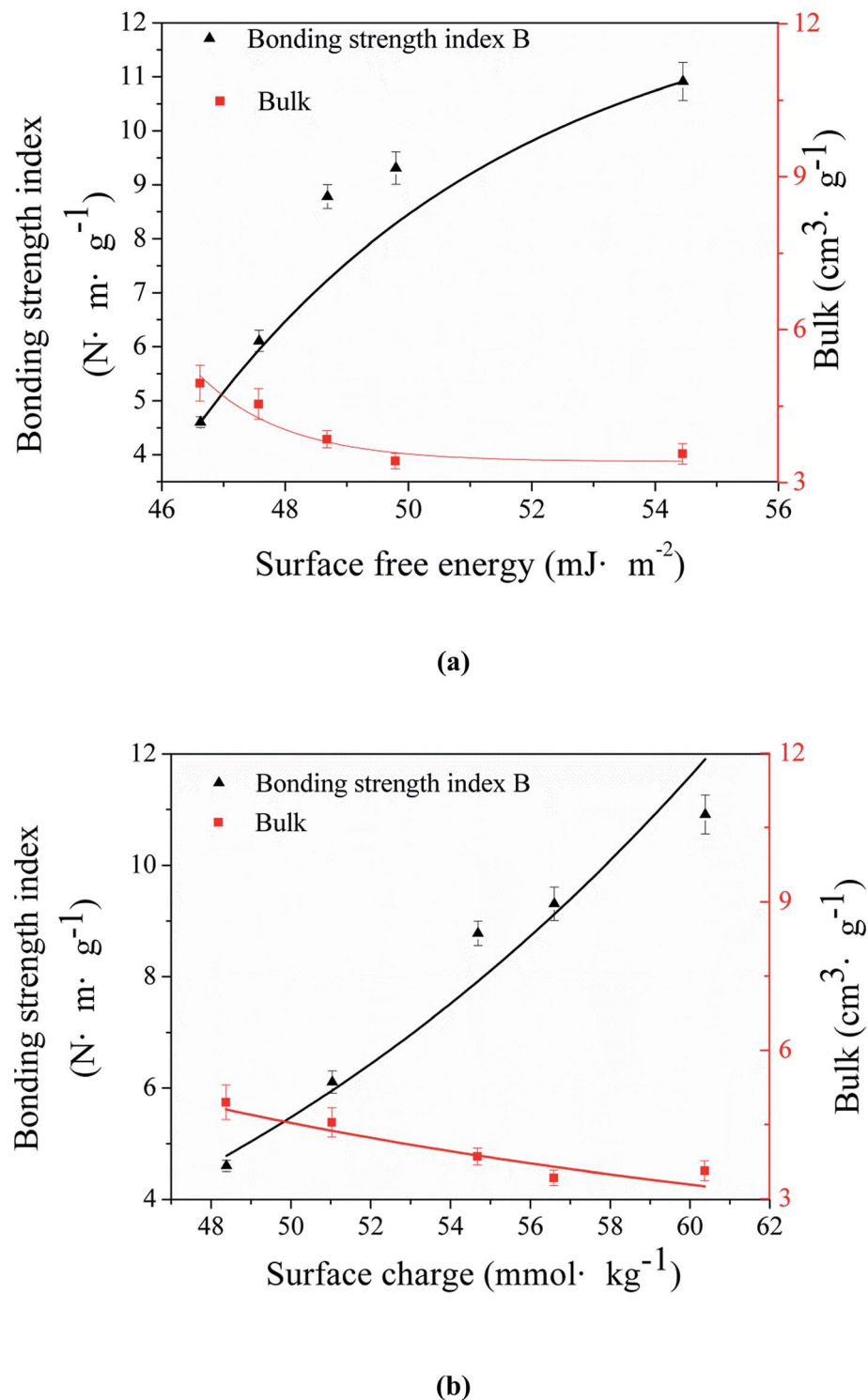


Fig. 6 Relationship between fiber surface wettability and bonding strength index and the bulk.

increase of surface functional groups such as hydroxyl groups and carboxyl groups. The increase of the surface free energy implies the increase of the surface hydrophilic groups, the main components of the hydrogen bonding between fibers. The increase of  $b$  with the improvement of surface charge and free energy points out that the surface wettability has a positive effect on the inter-fiber bonding of the final products.

### 3.4.3 Fiber surface wettability and bonding strength index ( $B$ ) and bulk.

The relationship between fiber surface wettability and bonding strength index ( $B$ ) and bulk is shown in Fig. 6.

It could be seen in Fig. 6(a) that the bonding strength index of the mechanically treated fibers increased from  $4.60 \text{ N m g}^{-1}$  to  $10.91 \text{ N m g}^{-1}$  with the improvement of the surface free energy, as the respect of the surface wettability. The fibers gain

a better inter bonding through the mechanical treatment mainly by increasing the fiber flexibility and specific surface area,<sup>26,28,44</sup> which is mainly caused by the decrease of the surface lignin.

Also, the relationship between the bonding strength index and the surface charge shows a similar result in Fig. 6(b). It's been confirmed that the improvement of the surface charge had a positive effect on the forming of the hydrogen bonding between fibers so that the bonding strength increased.

It's well-known that the bonding strength and the bulk are always a pair of contradiction, hard to compromise. However, in Fig. 6, the bulk only decreased a small deal (from  $4.95 \text{ cm}^3 \text{ g}^{-1}$  to  $3.56 \text{ cm}^3 \text{ g}^{-1}$ ) when the bonding strength index was increasing. This is because that most of the lignin was still retained in the fibers, which makes the fiber network hard enough and difficult to be squashed.<sup>45</sup> Above all, the improvement of the surface wettability can be useful for the balance between the bonding strength and the bulk of paper or paper-board products using lignin-rich lignin as raw materials.

## 4. Conclusion

Fiber surface wettability properties are vital for the inter-fiber bonding capability. During the mechanical treatment, the surface lignin decreased from 87.1% to 77.5%, so that the surface wettability was dramatically improved, including the surface charge increasing from  $48.38 \text{ mmol kg}^{-1}$  to  $60.38 \text{ mmol kg}^{-1}$  and the surface free energy rising from  $46.63 \text{ mJ m}^{-2}$  to  $54.45 \text{ mJ m}^{-2}$ .

Owing to the improvement of surface wettability, the fiber became more easily swelled and soften with more hydrophilic functional groups on the fiber surface, enhancing the RBA (from 125.53% to 130.12%) and  $b$  (from  $7.5 \text{ N m}^{-2}$  to  $11.3 \text{ N m}^{-2}$ ). However, the bulk of the lignin-rich fiber network decreased with the increase of the strength properties, which is not so obvious (from  $4.95 \text{ cm}^3 \text{ g}^{-1}$  to  $3.56 \text{ cm}^3 \text{ g}^{-1}$ ) with the increase of the surface wettability. It could be concluded that the modification of the surface wettability had a good effect on compromising the contradiction between the strength properties and the bulk property of the resulting products. Above all, with a good knowledge of surface wettability, both adjustably and measurably, the inter-fiber bonding strength can be positively changed and so can the bonding abilities between fibers and other materials.

## Conflicts of interest

There are no conflicts to declare.

## Acknowledgements

This work was supported by the National Natural Science Foundation of China (NSFC Grant No. 31670588; 31370577), and the China Postdoctoral Science Foundation (Grant No. 2016M600516).

## References

- R. Gaudreault, N. D. Cesare, T. G. M. V. D. Ven and D. A. Weitz, *Ind. Eng. Chem. Res.*, 2015, **54**, 6234–6246.
- X. Li and W. Strieder, *Ind. Eng. Chem. Res.*, 2009, **48**, 2236–2244.
- W. T. Tze and D. J. Gardner, *Wood Fiber Sci.*, 2001, **33**, 364–376.
- R. Yu, C. Wang and Y. Qiu, *Appl. Surf. Sci.*, 2007, **253**, 9283–9289.
- B. Wang, R. Li, B. He and J. Li, *BioResources*, 2011, **6**, 4356–4369.
- K. Kulasinski, D. Derome and J. Carmeliet, *J. Mech. Phys. Solids*, 2017, **103**, 221–235.
- T. Tabarsa, S. Sheykhanzari, A. Ashori, M. Mashkour and A. Khazaiean, *Int. J. Biol. Macromol.*, 2017, **101**, 334–340.
- C. Zhao, H. Zhang, X. Zeng, H. Li and D. Sun, *Cellulose*, 2016, **23**, 1617–1628.
- R. S. Ampulski, *Nord. Pulp Pap. Res. J.*, 1989, **4**, 155–163.
- E. Aracri, A. G. Barneto and T. Vidal, *Ind. Eng. Chem. Res.*, 2012, **51**, 3895–3902.
- M. Castellano, A. Gandini, P. Fabbri and M. N. Belgacem, *J. Colloid Interface Sci.*, 2004, **273**, 505–511.
- B. Ramalingam, B. Sana, J. Seayad, F. J. Ghadessy and M. B. Sullivan, *RSC Adv.*, 2017, **7**, 11951–11958.
- D. E. Rollings and J. G. C. Veinot, *Langmuir*, 2008, **24**, 13653–13662.
- K. Li and D. W. Reeve, *J. Pulp Pap. Sci.*, 2002, **28**, 369–373.
- H. Zhang, C. Zhao, Z. Li and J. Li, *Cellulose*, 2016, **23**, 163–173.
- S. L. Schellbach, S. N. Monteiro and J. W. Drelich, *Mater. Lett.*, 2016, **164**, 599–604.
- D. K. Owens and R. C. Wendt, *J. Appl. Polym. Sci.*, 1969, **13**, 1741–1747.
- Z. Li, H. Zhang, X. Wang, F. Zhang and X. Li, *RSC Adv.*, 2016, **6**, 109211–109217.
- B. Y. Wang and L. I. Rong, *China Pulp Pap. Ind.*, 2013, **12**, 33–36.
- I. Soszynski, *Nord. Pulp Pap. Res. J.*, 1995, **10**, 150–151.
- H. Hu, H. Li, Y. Zhang, Y. Chen, Z. Huang, A. Huang, Y. Zhu, X. Qin and B. Lin, *RSC Adv.*, 2015, **5**, 20656–20662.
- A. I. Adeogun, M. A. Idowu, K. O. Akiode and S. A. Ahmed, *Bioresources and Bioprocessing*, 2016, **3**, 1–16.
- P. Fardim and N. Durán, *Colloids Surf., A*, 2003, **223**, 263–276.
- N. K. Bhardwaj, V. Hoang and K. L. Nguyen, *Bioresour. Technol.*, 2007, **98**, 1647–1654.
- J. Li, Y. Liu, C. Duan, H. Zhang and Y. Ni, *Bioresour. Technol.*, 2015, **192**, 501–506.
- H. N. Banavath, N. K. Bhardwaj and A. K. Ray, *Bioresour. Technol.*, 2011, **102**, 4544–4551.
- Q. Miao, C. Tian, L. Chen, L. Huang, L. Zheng and Y. Ni, *Cellulose*, 2015, **22**, 803–809.
- L. O. Öhman, L. Wågberg, K. Malmgren and Å. Tjernström, *J. Pulp Pap. Sci.*, 1997, **23**, J467–J474.
- L. Paavilainen, *Pap. Puu*, 1993, **75**, 689–702.



30 G. V. Duarte, B. V. Ramarao, T. E. Amidon and P. T. Ferreira, *Ind. Eng. Chem. Res.*, 2011, **50**, 9949–9959.

31 J. Tao, H. Liu, J. Li, Z. Wu and W. Lv, *International Conference on Computer Engineering and Technology*, 2010, vol. 4, pp. 621–625.

32 L. Ming, H. Zhang, J. Li and J. Duan, *Ind. Eng. Chem. Res.*, 2013, **52**, 4083–4088.

33 A. Klash, E. Ncube, B. D. Toit and M. Meincken, *Eur. J. For. Res.*, 2010, **129**, 741–748.

34 M. A. Hubbe, R. A. Venditti and O. J. Rojas, *BioResources*, 2007, **2**, 739–788.

35 F. Fadavi, H. Kermanian and H. Resalati, *Lignocellulose*, 2012, **1**, 153–163.

36 X. Tang, X. Guo and K. Sun, *Advanced Textile Technology*, 2013, **21**, 57–59.

37 J. Simola, P. Malkavaara, R. Alén and J. Peltonen, *Polymer*, 2000, **41**, 2121–2126.

38 A. Haridas, C. Sharma, V. Sritharan and T. Rao, *RSC Adv.*, 2014, **4**, 12188–12197.

39 S. Y. Yoon and Y. Deng, *Ind. Eng. Chem. Res.*, 2007, **46**, 4883–4890.

40 G. Wang, A. M. Huang, X. X. Hu and F. M. Chen, *Guangpuxue Yu Guangpu Fenxi*, 2010, **30**, 2365–2367.

41 J. Tao, H. Liu, X. Chen, W. Shen and X. Zhu, *Paper Science & Technology*, 2007, **26**, 1–5.

42 K. L. Kato and R. E. Cameron, *Cellulose*, 1999, **6**, 23–40.

43 S. Fujisawa, Y. Okita and H. Fukuzumi, *Carbohydr. Polym.*, 2011, **84**, 579–583.

44 K. Grundke, K. Pöschel, A. Synytska, R. Frenzel, A. Drechsler, M. Nitschke, A. L. Cordeiro, P. Uhlmann and P. B. Welzel, *Adv. Colloid Interface Sci.*, 2015, **222**, 350–376.

45 D. Yan and K. Li, *J. Mater. Sci.*, 2008, **43**, 2869–2878.

